Journal of Electron Spectroscopy and Related Phenomena 250 (2021) 147085

Contents lists available at ScienceDirect

Journal of Electron Spectroscopy and Related Phenomena

journal homepage: www.elsevier.com/locate/elspec

Experimental evidence for a metastable state in $FeTe_{1-x}Se_x$ following coherent-phonon excitation

L.X. Yang [a,b], G. Rohde [c], Y.J. Chen [a], W.J. Shi [d,e], Z.K. Liu [d,f], F. Chen [g], Y.L. Chen [a,d,h,i], K. Rossnagel [c,j], M. Bauer [c,*]

[a] State Key Laboratory of Low Dimensional Quantum Physics, Department of Physics, Tsinghua University, Beijing 100084, PR China
[b] Frontier Science Center for Quantum Information, Beijing 100084, PR China
[c] Institut für Experimentelle und Angewandte Physik, Christian-Albrechts-Universität zu Kiel, D-24098 Kiel, Germany
[d] School of Physical Science and Technology, ShanghaiTech University and CAS-Shanghai Science Research Center, Shanghai 200031, PR China
[e] Max Planck Institute for Chemical Physics of Solids, D-01187 Dresden, Germany
[f] ShanghaiTech Laboratory for Topological Physics, Shanghai 200031, PR China
[g] Physics Department, Shanghai University, Shanghai 200031, PR China
[h] ShanghaiTech Laboratory for Topological Physics, Shanghai 200031, PR China
[i] Department of Physics, Clarendon Laboratory, University of Oxford, Oxford OX1 3PU, UK
[j] Ruprecht-Haensel-Labor, Deutsches Elektronen-Synchrotron DESY, D-22607 Hamburg, Germany

A B S T R A C T

Changes of the electronic structure of $FeTe_{1-x}Se_x$ (x = 0, 0.3) upon ultrafast excitation with near-infrared laser pulses are investigated using time- and angle-resolved extreme ultraviolet photoemission spectroscopy. At different temperatures and for different doping levels we observe a global oscillation of energy bands near the Fermi energy driven by the coherent excitation of the A_{1g}(Te) phonon mode in $FeTe_{1-x}Se_x$. Prominently, photo-induced band shifts and a spectral weight reduction persist for at least 300 ps, long after the decay of the photo-excited carriers and the damping of the coherent phonons. We argue that the system escapes from the original equilibrium state and is transiently trapped in a possibly metastable state envisioning a purely optical means of manipulating the electronic structure in an iron-based superconductor.

Ultrafast laser pulses possess the unique capability to coherently and selectively excite specific phonon modes, which not only provides rare opportunities to investigate crucial lattice dynamics, but also promises coherent control of electronic properties of quantum materials [1–12]. Coherent phonons and their interaction with other elementary excitations have been frequently studied using different types of quantitative pump–probe spectroscopies. These techniques are particularly useful in the investigation of quantum materials with strong electron–phonon coupling, in which a transient displacement of an atomic nucleus driven by a lattice vibration is directly linked to changes of the electronic structure via the deformation potential parameter [5–9,12–15].

In addition, photoexcitation can non-thermally excite the many-body ground state and bring the system into intriguing non-equilibrium states providing a purely optical control of the macroscopic state and physical properties of quantum materials [15–27]. During the relaxation process, the system can fall into novel states that are not accessible by thermal excitation. Such photo-induced metastable states can persist over long time periods and have been observed in electronic materials with competing quantum phases before, such as persistent low-temperature metallic phases out of charge-ordered insulating manganites [28,29], spontaneously ordered hidden states in transition-metal chalchogenides [30,31], and photo-induced conducting and high-temperature superconducting states in cuprates [32,33] and iron-based superconductors [34].

Upon photoexcitation of the coherent A_{1g}(Te) phonon mode, using time- and angle-resolved photoemission spectroscopy (trARPES), we study in the present work transient changes of the electronic structure in the iron-based superconductor (Fe-SC) $FeTe_{1-x}Se_x$. The experimental data reveal a phonon-driven oscillatory response of the electronic system in qualitative agreement with findings in other Fe-SC compounds [4–9,35,36]. More importantly, after the decay of the photo-generated hot carrier population and the damping of the coherent phonon mode we observe a persistent band shift and spectral weight suppression lasting much longer than 300 ps, the maximum time delay that can be probed with our experimental setup. It is argued that out of the coherent excitation of the A_{1g}(Te) mode a long-lived state of $FeTe_{1-x}Se_x$ is

* Corresponding author.
E-mail addresses: lxyang@tsinghua.edu.cn (L.X. Yang), bauer@physik.uni-kiel.de (M. Bauer).

https://doi.org/10.1016/j.elspec.2021.147085
Received 26 March 2021; Received in revised form 4 May 2021; Accepted 19 May 2021
Available online 24 May 2021

transiently stabilized that is characterized by a new, metastable equilibrium position of the Te atoms. The results emphasize the crucial role of the iron-chalcogen and iron-pnictogen bond length in Fe-SCs, respectively, which are known to be key parameters governing the superconducting and magnetic properties of this class of compounds [37]. They also suggest a purely optical and coherent method for controlling the electronic structure and macroscopic state of Fe-SCs.

High-quality $FeTe_{1-x}Se_x$ single crystals were grown by a self-flux method [38]. High-resolution static ARPES measurements were performed at beamline 5-4 at Stanford Synchrotron Radiation Lightsource (SSRL) using a Scienta R4000 analyzer with an energy resolution of about 15 meV. trARPES experiments were performed using a 8.2 kHz Ti: sapphire amplifier system (Dragon, KMLabs) (1 mJ pulse energy, 780 nm center wavelength) and a SPECS Phoibos 150 analyzer [42,43]. Sample surfaces were excited with 30-fs near-infrared (780 nm) pulses at an absorbed pump fluence of ~0.55 mJ/cm^2 and probed with 10-fs extreme-ultraviolet (XUV) HHG pulses at 22.1 eV [Fig. 1(a)] generated by the second harmonic of the amplifier output in an argon-filled hollow-fiber waveguide (XUUS, KMLabs). The effective time and energy resolutions in the trARPES experiment were 35 fs and 260 meV, respectively. The first-principles electronic structure calculations were carried out by using the projector augmented wave (PAW) method [39] as implemented in the VASP package [40]. The generalized gradient approximation (GGA) of Perdew–Burke–Ernzerhof (PBE) [41] was employed for the exchange-correlation functional. The kinetic energy cutoff of the plane-wave basis was set to be 400 eV. The experimental lattice constants and atomic positions were adopted. A 10 x 10 x 6 k-point mesh was used for sampling the Brillouin zone (BZ).

Fig. 1(a) schematically illustrates the coherent excitation of the A_{1g}(Te) phonon mode in the investigated FeTe systems and the detection of the subsequent changes in the electronic structure. Absorption of the pump pulse generates hot electrons and triggers at the same time a displacive excitation of the Te atoms, which start to oscillate coherently around the new equilibrium position of the excited-state potential energy surface. Changes in the electronic structure driven by the excitation

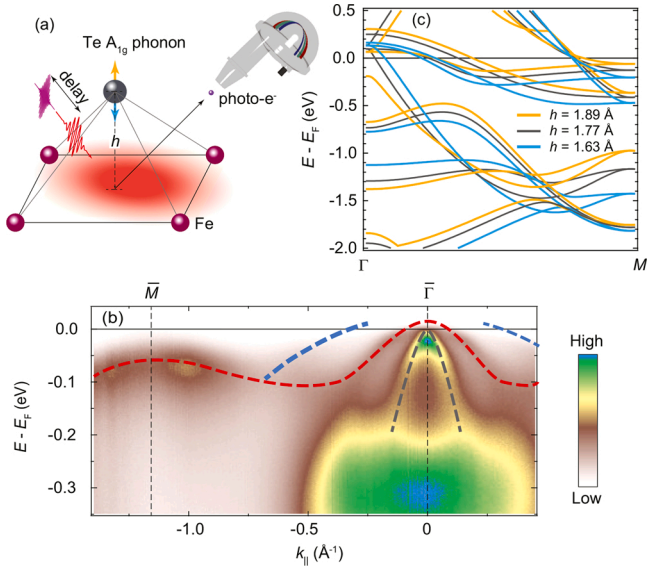

Fig. 1. Experiment and band structure of $FeTe_{1-x}Se_x$. (a) Schematic illustration of the trARPES experiment. The blue and orange arrows indicate the excitation of the coherent A_{1g}(Te) phonon mode. Distance h between a Te atom and the Fe-atom plane is indicated. (b) Band map of $FeTe_{0.7}Se_{0.3}$ along the $\overline{\Gamma M}$ direction as obtained with high-resolution ARPES. Dashed lines indicate the observed band dispersions. High-resolution ARPES data were taken at 15 K with *s*-polarized 22 eV photons. (c) Calculated band structure of FeTe along the ΓM direction computed as a function of h. (For interpretation of the references to color in this figure legend, the reader is referred to the web version of this article.)

of this phonon mode are monitored by trARPES using time-delayed XUV probe pulses. Fig. 1(b) shows the band structure of $FeTe_{0.7}Se_{0.3}$ along the $\overline{\Gamma M}$ direction obtained by static high-resolution ARPES (HHG-ARPES spectra at $\overline{\Gamma}$ and $\overline{M}$ are shown for comparison in the supplementary material, Fig. S1 [44]). We resolve three hole-like bands near the Fermi energy E_F around the $\overline{\Gamma}$ point and a hole-like band below E_F around the $\overline{M}$ point. The data are in very good agreement with results of previous ARPES measurements and *ab initio* calculations [38] except for the electron bands crossing the Fermi level near the $\overline{M}$ point, which in the present study are not resolved due to matrix-element effects. Our data also confirm the qualitative agreement with *ab initio* band structure calculations [see Ref. [38] and Fig. 1(c)]. The obvious quantitative mismatch in band width is due to correlation effects in this material. A scaling factor of around 3 between experiment and theory has been reported before [38].

Fig. 2(a) and (b) shows the pump-induced temporal evolution of trARPES spectra of FeTe at the $\overline{\Gamma}$ and $\overline{M}$ points. After the arrival of the pump pulse, we observe the instantaneous generation of a hot electron population above E_F and a strong spectral weight suppression below E_F followed by pronounced oscillations of the spectral weight, which is particularly visible in the close vicinity of E_F. The oscillations at $\overline{\Gamma}$ and $\overline{M}$ are in-phase and their period of 4.7 ± 0.2 THz corresponds to the frequency of the A_{1g}(Te) phonon mode [45]. Fig. 2(c) and (d) compares energy distribution curves (EDCs) at selected pump–probe delays Δt before and after excitation near $\overline{\Gamma}$ and $\overline{M}$. The data show that at least part of the oscillations arise from shifts of EDC band peaks suggesting that we probe here a modulation of the electronic band structure of FeTe due to electron–phonon coupling [7–9].

The in-phase oscillations are also clearly observed as modulations in the ARPES intensity: Fig. 3(a) and (b) shows ARPES intensity transients at $\overline{\Gamma}$ and $\overline{M}$ and for different sample base temperatures derived from an integration over an energy window of 500 meV below E_F. Further data show that the A_{1g}(Te) oscillations are universally observed for all temperatures and doping levels investigated in the present study [44].

We fit the ARPES intensity transients $I(t)$ shown in Fig. 3(a) and (b) using the following expression [44]:

$$I(t) = A_0 cos(\omega_A t + \phi_A) e^{-t/\tau_A} - B_0 e^{-t/\tau_B} - C_0,$$

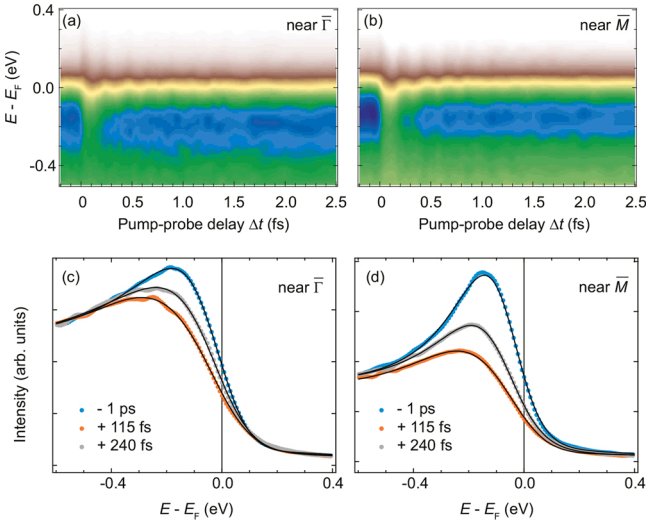

Fig. 2. Temporal evolution of ARPES spectra of FeTe. (a), (b) EDC transients near $\overline{\Gamma}$ and $\overline{M}$. (c), (d) Comparison of EDCs taken near $\overline{\Gamma}$ and $\overline{M}$ at selected pump–probe delays. Solid lines represent best fits with the model described in the text. trARPES data were taken at 30 K with *s*-polarized 22.1 eV probe pulses. Photoemission intensities in (a)–(d) were integrated over a momentum window of 0.2 Å^{-1} centered around the high-symmetry points.

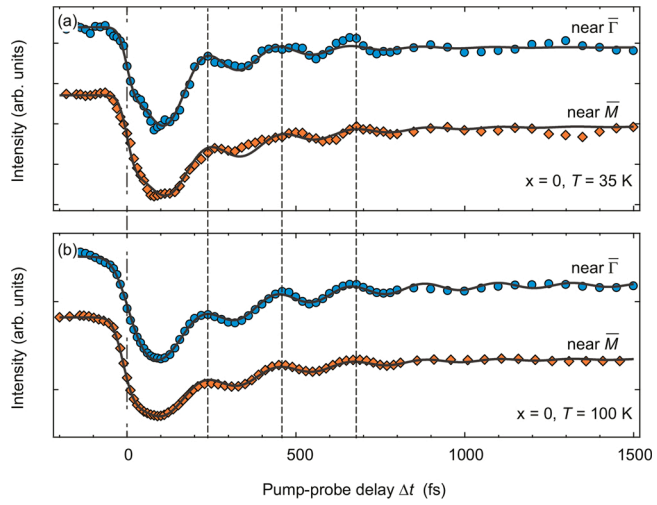

Fig. 3. ARPES intensity transients of FeTe as a function of Δt as obtained at 35 K (a) and 100 K (b). ARPES intensities were integrated over an energy window [−0.5, 0] eV below E_F. The solid black curves are fits to the data using the model described in the main text.

where A_0 and B_0 (τ_A and τ_B) represent the amplitudes (time constants) of the damped oscillation and exponential decay. The parameters ω_A and ϕ_A are the frequency and initial phase of the oscillation. The constant C_0 accounts for the residual offset in signal intensity observed for long delays. The finite time resolution of about 35 fs is taken into account by a Gaussian convolution. As can be seen in Fig. 3(a) and (b) the model reproduces the ARPES intensity transients reasonably well. The fit yields an initial phase of $\phi_A \approx (-0.05 \pm 0.025)\pi$, consistent with a displacive excitation of the coherent phonon. Changes in the A_{1g}(Te) oscillation period with temperature or doping level, as previously reported in a Raman scattering study [45], could not be resolved due to the limited time resolution of our experiment. However, the observed temperature dependence of the oscillation amplitude and damping rate [44] qualitatively resembles the findings in Ref. [45] and suggests an influence of the initial chalcogen height on the excitation and damping of the A_{1g}(Te) phonon mode [46].

For a quantitative evaluation of the observed shifts in the EDC peak positions, we approximated the transient EDCs with a Lorentzian plus a constant background, multiplied by a Fermi-Dirac function and convoluted with a Gaussian that accounts for the experimental resolution [44]. As shown in Fig. 2(c) and (d), the model well reproduces the experimental data. In a related study of $BaFe_2As_2$, we reported on a periodic modulation of the effective chemical potential μ in response to the excitation of the A_{1g} phonon mode [8]. The fits to the EDCs in the present work provide no evidence for similar effects in $FeTe_{1-x}Se_x$, at least within the resolution of the experiment. This observation either implies only a weak dependence of μ on the A_{1g}(Te) displacement amplitude or an effective electronic equilibration of the excited surface area with the bulk on timescales much faster than the A_{1g} oscillation period.

The spectral response to the excitation of the A_{1g}(Te) mode can qualitatively be understood with the help of *ab initio* calculations of the electronic structure as a function of the distance h between the Te and Fe planes. As can be seen in Fig. 1(c), small variations in the tellurium height h above the iron plane yield significant band shifts all over the Brillouin zone. Since the electrons respond much faster than the lattice, the electronic states will synchronize with the motion of the atomic nuclei, establishing an ultrafast oscillation of the electronic structure driven by the coherent excitation of the A_{1g}(Te) phonon mode. A direct comparison of the spectral shift observed at $\overline{\Gamma}$ with the calculated results is not meaningful: even though the high-resolution ARPES data imply that close to E_F the spectral weight is dominated by a single band (the inner hole-like band), the limited energy resolution of the trARPES experiment strongly mixes this signal with the next lower lying band (Fig. S1(a) [44]). According to the calculation the two bands oscillate out-of-phase and it is not possible to disentangle in the experimental data which of the two bands is finally responsible for the oscillatory behavior in the peak position. The situation at $\overline{M}$ is in contrast much clearer: the ARPES signal shows a single band, which due to its dispersion can be assigned to the hole-like band near E_F in Fig. 1(c) (see also [38]). From the initial increase in the binding energy of the band right after excitation and considering the theory results for different distances between the Te-atom and Fe-atom planes shown in Fig. 1(c) we conclude that the excited-state potential energy surface initially *reduces* the equilibrium distance h. Notably, for FeSe and $BaFe_2As_2$ time-resolved X-ray diffraction measurements reported an initial increase of the chalcogen and pnictogen height, respectively, upon coherent excitation of the A_{1g} mode [5–7]. This anti-phase behavior could be related to the rather large value of h in FeTe, which exceeds the corresponding value in FeSe and $BaFe_2As_2$ by approximately 25% [47].

Prominently, after the damping of the A_{1g}(Te) phonon mode we observe a persistent shift in the EDC peak position and a reduction in the ARPES intensity in comparison to the thermal equilibrium state probed in the experiment at $\Delta t < 0$ fs. The significance of spectral shift and signal reduction is illustrated in Fig. 4(a) and (b) which compares EDCs recorded near the $\overline{\Gamma}$ and $\overline{M}$ points at $\Delta t = -1$ ps and $\Delta t = 300$ ps. Fig. 4(c) and (d) present the temporal evolution of spectral weight and spectral shift up to $\Delta t = 300$ ps, the maximum delay that can be probed in our

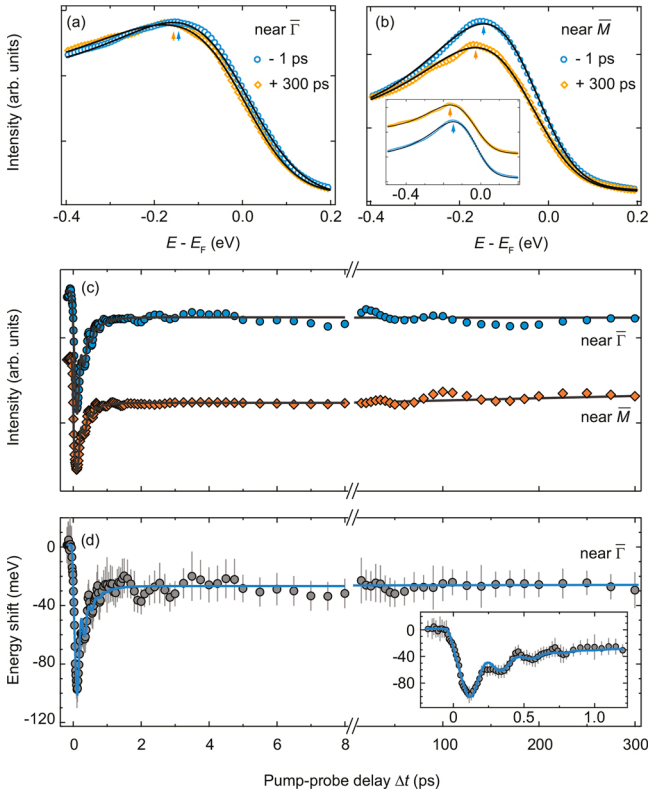

Fig. 4. Long-term transient spectral changes observed for FeTe. (a), (b) EDCs recorded at $\Delta t = -1$ ps and $\Delta t = 300$ ps near $\overline{\Gamma}$ and $\overline{M}$, respectively. The inset of panel (b) shows the same data normalized to the peak maximum and plotted with an offset for better visibility of the peak shift near $\overline{M}$. The orange and blue arrows indicate the maxima positions of the EDC peaks. Solid lines represent best fits with the model described in the text. (c) Temporal evolution of the ARPES intensity near $\overline{\Gamma}$ up to $\Delta t = 300$ ps. Data were obtained by integrating the transient EDCs over an energy window [−0.5, 0] eV below E_F. (d) Shift in band peak energy as a function of Δt obtained by fitting the EDCs with the model described in the text. Solid lines in (c) and (d) are fits to the data to guide the eye. Data were taken at 35 K.

experiment. After the damping of the A_{1g}(Te) phonon mode and within the probed time delay, both, spectral weight suppression and spectral shift do virtually not change any more (see the supplementary material for spectral shift data at $\overline{M}$ [44]). However, on timescales of the repetition rate of the laser (122 μs) the spectrum has fully recovered into the initial state again. The transient and long-lived spectral changes are observed over the entire BZ, suggesting a global and metastable modulation of the electronic structure of FeTe. The persistence of the spectral weight suppression and spectral shift on the probed timescales implies the lifetime of this modulation being at least far in the nanosecond range.

We exclude purely thermal effects due to lattice heating being the origin of these long-term changes: For a direct comparison we performed static ARPES experiments at different sample base temperatures T_0 using the HHG-based trARPES setup. The results clearly show that the thermally induced spectral changes observed under equilibrium conditions do quantitatively and qualitatively not match the long-term spectral changes observed upon photoexcitation. Fig. 5 compares the relative changes in the ARPES intensity at $\overline{\Gamma}$, $\Delta I/I(T_0)$, upon photoexcitation and thermal excitation. For the photoexcitation case we calculate $\Delta I/I(T_0)$ from data recorded at $\Delta t = 300$ ps and $\Delta t = -1$ ps. A fit of a three-temperature model to electron-temperature transients derived from the trARPES data indicates for $T_0 = 35$ K a pump-induced increase of the lattice temperature of <50 K at 300 ps [44]. For the thermal equilibrium reference we therefore calculate $\Delta I/I(T_0)$ from data recorded at the sample base temperatures T_0 and $T_0 + 50$ K. Note that the thermal equilibrium values of $\Delta I/I(T_0)$ for sample base temperatures $T_0 > 35$ K yield an upper limit for the thermally induced changes that can contribute at $\Delta t = 300$ ps as the specific heat of the sample increases with temperature [46]. Over most of the probed temperature range the thermal equilibrium values of $\Delta I/I(T_0)$ are significantly smaller than the corresponding data associated with the metastable state and stay at around 1–2%. Only in the temperature range between 75 and 120 K the analysis of equilibrium and non-equilibrium data sets yield very similar values with the equilibrium data showing a very pronounced discontinuity in the temperature dependence. We tentatively associate this discontinuity with the melting of the SDW phase of FeTe at $T = 75$ K and, at higher temperatures, with the thermal destruction of SDW fluctuations. In contrast to the thermal response of the system, the photoexcitation data show a continuous behavior with relative changes in the ARPES intensity ranging between 4% and 9% in the probed temperature range. Notably, the relative changes seem to saturate at low temperatures and decrease above 120 K, where the high-temperature discontinuity occurs in the thermal equilibrium data.

Additionally, the temperature dependence of the spectral weight suppression at long delays shows no correlation with the temperature dependence of the specific heat of FeTe [46], but a saturation below 120 K, further excluding a dominating contribution of thermal effects to the long-lived spectral change. Interestingly, the saturation of the long-lived signal mimics the saturated lattice shrinkage of FeTe at low temperatures reported in Ref. [48], which points to a close relationship between the long-lived signal and a lattice change. In contrast, the static ARPES signal shows no saturation behavior in its temperature dependence.

The distinct difference between thermal response and photoexitation suggests that the long-lived signal is related to the formation of a metastable state of FeTe that cannot be prepared under equilibrium conditions. Inspired by the smooth crossover from the coherent modulations in the trARPES spectra to the long-lived spectral changes, we propose that the metastable state evolves out of the non-thermal excited state initially prepared by the absorption of the pump pulse. The observed band shift toward higher binding energies in comparison to the positive deformation potential as predicted by our band structure calculations implies that in the metastable state the Te atoms are trapped at a distance from the iron plane that is different from the one in the equilibrium ground state.

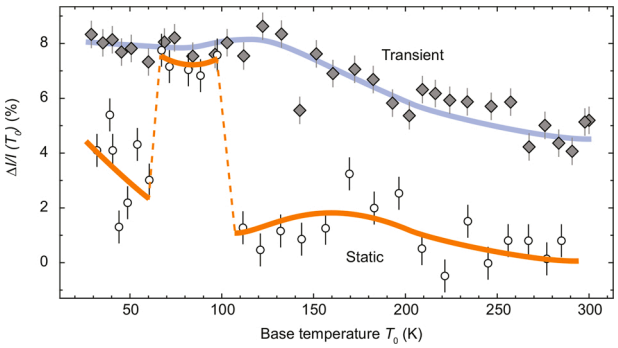

Fig. 5. Temperature dependence of the spectral changes at long delays. Comparison of the relative changes in the ARPES intensity at $\overline{\Gamma}$ in response to photoexcitation (solid diamonds) and thermal excitation (open circles) as a function of the sample base temperature T_0. The photo-induced (transient) data points correspond to the relative changes in the ARPES intensity of spectra recorded at $\Delta t = -1$ ps and $\Delta t = 300$ ps. The static spectral changes were obtained from the comparison of ARPES data recorded at T_0 and $T_0 + 50$ K using the same trARPES setup. ARPES intensities were integrated over an energy window [−0.5, 0] eV below E_F. The blue and orange curves are guides to the eyes for the spectral changes. (For interpretation of the references to color in this figure legend, the reader is referred to the web version of this article.)

Finally, although the results of band structure calculations as shown in Fig. 1(c) provide a hint for understanding the long-lived spectral changes, the nature of the possible metastable state remains unclear. Previous calculated results showed that the antiferromagnetic double-stripe ground state of FeTe is highly susceptible to changes in the chalcogen height h. Already minor changes in h are predicted to drive the system into either an antiferromagnetic single-stripe phase or a ferromagnetic phase [49,50]. This is in contrast to FeSe, in which the antiferromagnetic ground state is expected to be much more robust against changes in h. It is also noteworthy that our data show general agreement with a recent study of $FeTe_{0.6}Se_{0.4}$ that reported on the observation of a metastable state associated with the transient formation of a nematic phase [52]. Since the long-lived signal is intimately related to the excitation and relaxation of coherent phonons in the system, one could speculate whether the chalcogen height h is a key parameter to control the nematic phase in the phase diagram of $FeTe_{1-x}Se_x$. FeTe is also known to be a phase-change material which can be switched from a crystalline phase to an anomalous amorphous phase upon illumination with nanosecond laser radiation [51]. All these aspects could play a critical role in the formation of the observed metastable state in FeTe. Further experimental and theoretical efforts are, however, necessary to gain more detailed insights into the nature and origin of the metastable state.

In conclusion, in a trARPES study of $FeTe_{1-x}Se_x$ we observed persistent and global spectral changes that emerge from an oscillatory response of the electronic structure to the coherent excitation of the A_{1g}(Te) phonon mode. The spectral changes remain virtually constant at least over a time period of 300 ps hinting at the formation of a metastable state. Our results not only shed light on relevant microscopic interactions in iron-based superconductors, but also suggest a promising means of manipulating electronic structure and magnetic properties of $FeTe_{1-x}Se_x$ calling for further research efforts.

Declaration of Competing Interest

The authors report no declarations of interest.

Acknowledgements

This work was supported by the National Science Foundation of

China (NSFC) through project 11774190, the Ministry of Science and Technology of China through project 2017YFA0304600, and the German Research Foundation (DFG) through project BA 2177/10-1. L.X. Y. acknowledges support from Tsinghua University Initiative Scientific Research Program. W.S. acknowledges support from the Shanghai high repetition rate XFEL and extreme light facility (SHINE).

Appendix A. Supplementary data

Supplementary data associated with this article can be found, in the online version, at https://doi.org/10.1016/j.elspec.2021.147085.

References

[1] F. Schmitt, P.S. Kirchmann, U. Bovensiepen, R.G. Moore, L. Rettig, M. Krenz, J.-H. Chu, N. Ru, L. Perfetti, D.H. Lu, M. Wolf, I.R. Fisher, Z.X. Shen, Science 321 (2008) 1649.
[2] M. Hase, P. Fons, K. Mitrofanov, A.V. Kolobov, J. Tominaga, Nat. Commun. 6 (2015) 8367.
[3] R. Yusupov, T. Mertelj, V.V. Kabanov, S. Brazovskii, P. Kusar, J.-H. Chu, I.R. Fisher, D. Mihailovic, R. Yusupov, Nat. Phys. 6 (2010) 681.
[4] K.W. Kim, A. Pashkin, H. Schäfer, M. Beyer, M. Porer, T. Wolf, C. Bernhard, J. Demsar, R. Huber, A. Leitenstorfer, Nat. Mater. 11 (2012) 497.
[5] L. Rettig, S.O. Mariager, A. Ferrer, S. Grübel, J.A. Johnson, J. Rittmann, T. Wolf, S. L. Johnson, G. Ingold, P. Beaud, U. Staub, Phys. Rev. Lett. 114 (2015) 067402.
[6] S. Gerber, K.W. Kim, Y. Zhang, D. Zhu, N. Plonka, M. Yi, G.L. Dakovski, D. Leuenberger, P.S. Kirchmann, R.G. Moore, M. Chollet, J.M. Glownia, Y. Feng, J.-S. Lee, A. Mehta, A.F. Kemper, T. Wolf, Y.-D. Chuang, Z. Hussain, C.-C. Kao, B. Moritz, Z.-X. Shen, T.P. Devereaux, W.-S. Lee, Nat. Commun. 6 (2015) 7377.
[7] S. Gerber, S.-L. Yang, D. Zhu, H. Soifer, J.A. Sobota, S. Rebec, J.J. Lee, T. Jia, B. Moritz, C. Jia, A. Gauthier, Y. Li, D. Leuenberger, Y. Zhang, L. Chaix, W. Li, H. Jang, J.-S. Lee, M. Yi, G.L. Dakovski, S. Song, J.M. Glownia, S. Nelson, K.W. Kim, Y.-D. Chuang, Z. Hussain, R.G. Moore, T.P. Devereaux, W.-S. Lee, P.S. Kirchmann, Z.-X. Shen, Science 357 (2017) 71.
[8] L.X. Yang, G. Rohde, T. Rohwer, A. Stange, K. Hanff, C. Sohrt, L. Rettig, R. Cortés, F. Chen, D.L. Feng, T. Wolf, B. Kamble, I. Eremin, T. Popmintchev, M.M. Murnane, H.C. Kapteyn, L. Kipp, J. Fink, M. Bauer, U. Bovensiepen, K. Rossnagel, Phys. Rev. Lett. 112 (2014) 207001.
[9] L. Rettig, R. Cortes, S. Thirupathaiah, P. Gegenwart, H.S. Jeevan, M. Wolf, J. Fink, U. Bovensiepen, Phys. Rev. Lett. 108 (2012) 097002.
[10] C.P. Weber, M.G. Masten, T.C. Ogloza, B.S. Berggren, M.K.L. Man, K.M. Dani, J. Liu, Z. Mao, D.D. Klug, A.A. Adeleke, Y. Yao, Phys. Rev. B 98 (2018) 155115.
[11] T. Shimojima, Y. Suzuki, A. Nakamura, N. Mitsuishi, S. Kasahara, T. Shibauchi, Y. Matsuda, Y. Ishid, S. Shin, K. Ishizaka, Nat. Commun. 10 (2019) 1946.
[12] E. Papalazarou, J. Faure, J. Mauchain, M. Marsi, A. Taleb-Ibrahimi, I. Reshetnyak, A. van Roekeghem, I. Timrov, N. Vast, B. Arnaud, L. Perfetti, Phys. Rev. Lett. 108 (2012) 256808.
[13] P.A. Loukakos, M. Lisowski, G. Bihlmayer, S. Blügel, M. Wolf, U. Bovensiepen, Phys. Rev. Lett. 98 (2007) 097401.
[14] D. Leuenberger, H. Yanagisawa, S. Roth, J.H. Dil, J.W. Wells, P. Hofmann, J. Osterwalder, M. Hengsberger, Phys. Rev. Lett. 110 (2013) 136806.
[15] L. Perfetti, P.A. Loukakos, M. Lisowski, U. Bovensiepen, H. Berger, S. Biermann, P. S. Cornaglia, A. Georges, M. Wolf, Phys. Rev. Lett. 97 (2006) 067402.
[16] A. Cavalleri, Th. Dekorsy, H.H.W. Chong, J.C. Kieffer, R.W. Schoenlein, Phys. Rev. B 70 (2004) 161102(R).
[17] A. Tomeljak, H. Schäfer, D. Städter, M. Beyer, K. Biljakovic, J. Demsar, Phys. Rev. Lett. 102 (2009) 066404.
[18] H. Schäfer, V.V. Kabanov, M. Beyer, K. Biljakovic, J. Demsar, Phys. Rev. Lett. 105 (2010) 066402.
[19] S. Wall, D. Brida, S.R. Clark, H.P. Ehrke, D. Jaksch, A. Ardavan, S. Bonora, H. Uemura, Y. Takahashi, T. Hasegawa, H. Okamoto, G. Cerullo, A. Cavalleri, Nat. Phys. 7 (2011) 114.
[20] T. Rohwer, S. Hellmann, M. Wiesenmayer, C. Sohrt, A. Stange, B. Slomski, A. Carr, Y.W. Liu, L.M. Avila, M. Kalläne, S. Mathias, L. Kipp, K. Rossnagel, M. Bauer, Nature 471 (2011) 490.
[21] J.C. Petersen, S. Kaiser, N. Dean, A. Simoncig, H.Y. Liu, A.L. Cavalieri, C. Cacho, I. C.E. Turcu, E. Springate, F. Frassetto, L. Poletto, S.S. Dhesi, H. Berger, A. Cavalleri, Phys. Rev. Lett. 107 (2011) 177402.
[22] C.L. Smallwood, J.P. Hinton, C. Jozwiak, W.T. Zhang, J.D. Koralek, H. Eisaki, D.-H. Lee, J. Orenstein, A. Lanzara, Science 336 (2012) 1137.
[23] S. Hellmann, T. Rohwer, M. Kalläne, K. Hanff, C. Sohrt, A. Stange, A. Carr, M. M. Murnane, H.C. Kapteyn, L. Kipp, M. Bauer, K. Rossnagel, Nat. Commun. 3 (2012) 1069.
[24] M. Porer, U. Leierseder, J.-M. Ménard, H. Dachraoui, L. Mouchliadis, I.E. Perakis, U. Heinzmann, J. Demsar, K. Rossnagel, R. Huber, Nat. Mater. 13 (2014) 857.
[25] V.R. Morrison, R.P. Chatelain, K.L. Tiwari, A. Hendaoui, A. Bruhács, M. Chaker, B. J. Siwick, Science 346 (2014) 445.
[26] M. Mitrano, A. Cantaluppi, D. Nicoletti, S. Kaiser, A. Perucchi, S. Lupi, P. Di Pietro, D. Pontiroli, M. Ricc, S.R. Clark, D. Jaksch, A. Cavalleri, Nature 530 (2016) 461.
[27] A. Kogar, A. Zong, P.E. Dolgirev, X.Z. Shen, J. Straquadine, Y.-Q. Bie, X.R. Wang, T. Rohwer, I.-C. Tung, Y.F. Yang, R.K. Li, J. Yang, S. Weathersby, S. Park, M. E. Kozina, E.J. Sie, H.D. Wen, P. Jarillo-Herrero, I.R. Fisher, X.J. Wang, N. Gedik, Nat. Phys. 16 (2019) 159.
[28] N. Takubo, Y. Ogimoto, M. Nakamura, H. Tamaru, M. Izumi, K. Miyano, Phys. Rev. Lett. 95 (2005) 017404.
[29] J. Zhang, X. Tan, M. Liu, S.W. Teitelbaum, K.W. Post, F. Jin, K.A. Nelson, D. N. Basov, W. Wu, R.D. Averitt, Nat. Mater. 15 (2016) 956.
[30] L. Stojchevska, I. Vaskivskyi, T. Mertelj, P. Kusar, D. Svetin, S. Brazovskii, D. Mihailovic, Science 344 (2014) 177.
[31] X. Shi, W.J. You, Y.C. Zhang, Z.S. Tao, P.M. Oppeneer, X.X. Wu, R. Thomale, K. Rossnagel, M. Bauer, H. Kapteyn, M. Murnane, Sci. Adv. 5 (2019) eaav4449.
[32] D. Fausti, R.I. Tobey, N. Dean, S. Kaiser, A. Dienst, M.C. Hoffmann, S. Pyon, T. Takayama, H. Takagi, A. Cavalleri, Science 331 (2011) 189.
[33] G. Yu, C.H. Lee, A.J. Heeger, N. Herron, E.M. McCarron, Phys. Rev. Lett. 67 (1991) 2581.
[34] T. Suzuki, T. Someya, T. Hashimoto, S. Michimae, M. Watanabe, M. Fujisawa, T. Kanai, N. Ishii, J. Itatani, S. Kasahara, Y. Matsuda, T. Shibauchi, K. Okazaki, S. Shin, Commun. Phys. 2 (2019) 115.
[35] B. Mansart, D. Boschetto, A. Savoia, F. Rullier-Albenque, A. Forget, D. Colson, A. Rousse, M. Marsi, Phys. Rev. B 80 (2009) 172504.
[36] H. Takahashi, Y. Kamihara, H. Koguchi, T. Atou, H. Hosono, I. Katayama, J. Takeda, M. Kitajima, K.G. Nakamura, J. Phys. Soc. Jpn. 80 (2011) 013707.
[37] D.C. Jonston, Adv. Phys. 59 (2010) 803.
[38] F. Chen, B. Zhou, Y. Zhang, J. Wei, H.W. Ou, J.F. Zhao, C. He, Q.Q. Ge, M. Arita, K. Shimada, H. Namatame, M. Taniguchi, Z.Y. Lu, J.P. Hu, X.Y. Cui, D.L. Feng, Phys. Rev. B 81 (2010) 014526.
[39] P.E. Blöchl, Phys. Rev. B 50 (1994) 17953.
[40] G. Kresse, J. Hafner, Phys. Rev. B 47 (1993) 558.
[41] J.P. Perdew, K. Burke, M. Ernzerhof, Phys. Rev. Lett. 77 (1996) 3865.
[42] S. Eich, A. Stange, A.V. Carr, J. Urbancic, T. Popmintchev, M. Wiesenmayer, K. Jansen, A. Ruffing, S. Jakobs, T. Rohwer, S. Hellmann, C. Chen, P. Matyba, L. Kipp, K. Rossnagel, M. Bauer, M.M. Murnane, H.C. Kapteyn, S. Mathias, M. Aeschlimanna, J. Electron Spectrosc. Relat. Phenom. 195 (2014) 231.
[43] G. Rohde, A. Hende, A. Stange, K. Hanff, L.-P. Oloff, L.X. Yang, K. Rossnagel, M. Bauer, Rev. Sci. Instrum. 65 (2016) 1853.
[44] See Supplementary Materials at https://doi.org/10.1016/j.elspec.2021.147085 for additional information on trARPES data and data analysis.
[45] V. Gnezdilov, Yu. Pashkevich, P. Lemmens, A. Gusev, K. Lamonova, T. Shevtsova, I. Vitebskiy, O. Afanasiev, S. Gnatchenko, V. Tsurkan, J. Deisenhofer, A. Loidl, Phys. Rev. B 83 (2011) 245127.
[46] A. Martinelli, A. Palenzona, M. Tropeano, C. Ferdeghini, M. Putti, M.R. Cimberle, T.D. Nguyen, M. Affronte, C. Ritter, Phys. Rev. B 81 (2010) 094115.
[47] L. Malavasi, S. Margadonna, Chem. Soc. Rev. 41 (2012) 3897.
[48] S.L. Bud'ko, P.C. Canfield, A.S. Sefat, B.C. Sales, M.A. McGuire, D. Mandrus, Phys. Rev. B 80 (2009) 134523.
[49] J. Kumar, S. Auluck, P.K. Ahluwalia, V.P.S. Awana, Supercond. Sci. Technol. 25 (2012) 095002.
[50] C.Y. Moon, H.J. Choi, Phys. Rev. Lett. 104 (2010) 057003.
[51] X.T. Fu, W.D. Song, H.W. Ho, R. Ji, L. Wang, M.H. Hong, Appl. Phys. Lett. 100 (2012) 201906.
[52] L. Fanfarillo, D. Kopić, A. Sterzi, G. Manzoni, A. Crepaldi, V. Tsurkan, D. Croitori, J. Deisenhofer, F. Parmigiani, M. Capone, F. Cilento, 2019. arXiv:1905:12448.